#104

Phys Chem Minerals (1986) 13:69–78

PHYSICS AND CHEMISTRY OF MINERALS

High-Pressure Crystal Chemistry of Phenakite (Be_2SiO_4) and Bertrandite ($Be_4Si_2O_7(OH)_2$)

Robert M. Hazen and Andrew Y. Au
Geophysical Laboratory, Carnegie Institution of Washington, Washington, DC 20008, USA

Abstract. Compressibilities and high-pressure crystal structures have been determined by X-ray methods at several pressures for phenakite and bertrandite. Phenakite (hexagonal, space group $R\bar{3}$) has nearly isotropic compressibility with $\beta = 1.60 \pm 0.03 \times 10^{-4}$ kbar^{-1} and $\beta = 1.45 \pm 0.07 \times 10^{-4}$ kbar^{-1}. The bulk modulus and its pressure derivative, based on a second-order Birch-Murnaghan equation of state, are 2.01 ± 0.08 Mbar and 2 ± 4, respectively. Bertrandite (orthorhombic, space group $Cmc2_1$) has anisotropic compression, with $\beta_a = 3.61 \pm 0.08$, $\beta_b = 5.78 \pm 0.13$ and $\beta_c = 3.19 \pm 0.10$ (all $\times 10^{-4}$ kbar^{-1}). The bulk modulus and its pressure derivative are calculated to be 0.70 ± 0.03 Mbar and 5.3 ± 1.5, respectively.

Both minerals are composed of frameworks of beryllium and silicon tetrahedra, all of which have tetrahedral bulk moduli of approximately 2 Mbar. The significant differences in linear compressibilities of the two structures are a consequence of different degrees of $T-O-T$ bending.

Introduction

Minerals in the system $BeO - Al_2O_3 - SiO_2$ provide an ideal test for various theoretical and empirical models of silicate behavior. The several binary and ternary phases in the system form large, relatively perfect, ordered, stoichiometric crystals in a variety of structures. All the constituent ions have relatively low atomic number and thus are amenable to the methods of computational quantum chemistry. Only three types of cation polyhedra – tetrahedral silicon, beryllium and octahedral aluminum – form the structural units for almost all the phases, thus providing an excellent test of the "polyhedral approach" (Hazen 1985). The present paper on high-pressure crystal chemistry of the beryllium orthosilicates and the following paper on phenakite elastic moduli (A. Yeganeh-Haeri and D.J. Weidner, in preparation), are part of a larger research program to document equations of state, elastic properties, vibrational spectra, thermochemistry and comparative crystal chemistry of these simple minerals.

The crystal structure of phenakite (Be_2SiO_4: hexagonal, $R\bar{3}$, $Z = 18$) was described by Zachariasen (1972) and by Downs (1983), both of whom reported anisotropic temperature parameters. The structure of bertrandite [$Be_4Si_2O_7(OH)_2$: orthorhombic, $Cmc2_1$, $Z = 4$] was refined by Solov'eva and Belov (1965), who presented isotropic thermal parameters. The close topological relationships between bertrandite, hemimorphite [$Zn_4Si_2O_7(OH)_2 \cdot H_2O$] and bromellite (BeO) were noted by Simonov and Belov (1976).

Among the objectives of the present investigation of beryllium orthosilicates are (1) to determine pressure-volume equation-of-state parameters, (2) to measure polyhedral bulk moduli and to test the hypothesis that polyhedral bulk moduli for a given type of cation polyhedron are similar from structure to structure, (3) to identify compression mechanisms in the beryllium orthosilicates, and (4) to provide a structural basis for interpreting the elastic moduli determined by Yeganeh-Haeri and Weidner (in preparation).

Experimental

Specimen Description

Crystals of natural phenakite from San Miguel di Piracicaba, Brazil (National Museum of Natural History No. B21152), and natural bertrandite from Albany, Maine (Field Museum of Natural History No. 6969), were provided by Mark Barton (Department of Geological Sciences, University of California at Los Angeles). Both minerals are colorless, transparent and visually free of defects; microprobe analysis of the samples by Barton (1985) revealed no significant chemical impurities. Crystal fragments of dimensions approximately $100 \times 100 \times 40$ μm were selected for X-ray diffraction studies at room and high pressure.

Data Collection at Room Pressure

Room-temperature lattice parameters for both minerals were refined from diffractometer angles of twenty reflections, each of which was measured in eight equivalent positions (King and Finger 1979). Values of 2θ ranged from 25 to 35° for phenakite and from 24 to 37° for bertrandite. Unit-cell parameters were refined without symmetry constraints (i.e., as triclinic). The observed cell dimensions of phenakite and bertrandite (Table 1) were consistent with hexagonal and orthorhombic symmetry, respectively.

Intensities of all reflections in a hemisphere of the sphere of reflection with ($\sin\theta/\lambda \leqq 0.7$ Å^{-1} were measured by an automated, four-circle diffractometer with monochromatized Mo$K\alpha$ radiation. Omega step scans with 0.025° step increments and 4-s counting time per step were used. Digi-

Table 1. Unit-cell parameters of phenakite (A) and bertrandite (B) at several pressures

A. Phenakite

Pressure (kbar)	a(Å)	c(Å)	V(Å^3)	c/a	V/V_0
0.001	12.4704 (9)[a]	8.2504 (6)	1111.1 (1)	0.6616	1.0000
13	12.440 (6)	8.233 (2)	1103.4 (10)	0.6618	0.9931 (9)
16	12.437 (4)	8.228 (1)	1102.3 (4)	0.6616	0.9921 (4)
25	12.419 (5)	8.220 (2)	1097.7 (9)	0.6619	0.9880 (9)
36	12.397 (3)	8.207 (1)	1092.4 (4)	0.6620	0.9832 (4)
37	12.393 (3)	8.204 (1)	1091.9 (3)	0.6620	0.9818 (3)
41	12.388 (3)	8.194 (2)	1089.0 (6)	0.6614	0.9801 (6)
49	12.370 (2)	8.188 (2)	1085.0 (4)	0.6619	0.9765 (4)

B. Bertrandite

Pressure (kbar)	a(Å)	b(Å)	c(Å)	V(Å^3)	V/V_0
0.001	8.7135 (4)	15.268 (1)	4.5683 (3)	607.74 (8)	1.0000
17.3	8.6559 (4)	15.107 (3)	4.5407 (3)	593.74 (13)	0.9770
23.0	8.641 (1)	15.051 (2)	4.5338 (6)	589.66 (13)	0.9703
35.2	8.6021 (6)	14.955 (7)	4.5157 (4)	580.9 (3)	0.9558
41.0	8.587 (1)	14.912 (2)	4.5901 (5)	577.54 (12)	0.9503

[a] Parenthesized figures represent *esd*'s

tized data for each step scan were converted to integrated intensities using the algorithm of Lehmann and Larsen (1974). Backgrounds were selected manually where necessary. Refinement conditions are given in Table 2 and refined isotropic extinction parameter (Zachariasen 1967) and structural parameters for Be_2SiO_4 and $Be_4Si_2O_7(OH)_2$ appear in Table 3. Refined anisotropic temperature parameters and the magnitudes and orientation of thermal vibration ellipsoids appear in Tables 4 and 5, respectively.

Data Collection at High Pressure

Flat, plate-like crystals approximately 40 μm thick were mounted in a diamond-anvil pressure cell for X-ray diffraction, with an alcohol mixture of 4:1 methanol:ethanol as the hydrostatic pressure medium and 5- to 10-μm chips of ruby as the internal pressure calibrant. Pressure-cell design, loading, operation and calibration are described by Hazen and Finger (1982). Special care was taken to avoid X-ray shielding by the gasket portions of the diamond cell. Large gasket holes of 400 μm were employed and the 100-μm crystals were well centered throughout the experiments.

Lattice constants of the two beryllium silicates were determined at several pressures. From 12 to 20 reflections were measured by the method of Hamilton (1974), as modified by King and Finger (1979), in order to correct for errors in crystal centering and diffractometer alignment. The same classes of reflection used to determine unit-cell parameters at room pressure were used in the high-pressure unit-cell measurements. Each set of angular data was refined without constraint and the resultant "triclinic" cell was examined for conformity with expected hexagonal and orthorhombic symmetries of phenakite and bertrandite, respectively. These symmetry conditions were met within two standard deviations at all pressures studied. This behavior is evidence that nearly hydrostatic conditions were maintained during the experiments. High-pressure unit-cell parameters are recorded in Table 1.

Intensity data for three-dimensional structure refinements were collected on all accessible reflections with $(\sin\theta)/\lambda \leqq 0.7$. Unusually short omega increments (0.02°) and long counting times (from 8 to 10 s per increment) were employed to optimize the number of observed reflections and the precision of those reflections. (Tabulated observed and calculated structure factors for phenakite at four pressures and bertrandite at three pressures are available from the authors on request.) The fixed-ϕ mode of data collection was used to maximize reflection accessibility and minimize attenuation by the diamond cell and a correction was made for X-ray absorption by the diamond and beryllium components of the pressure cell (Hazen and Finger 1982). Conditions of high-pressure refinements as well as refined atomic positional parameters and isotropic thermal parameters are recorded in Tables 2 and 3.

Results

Room-Pressure Structures

Refined atomic positional parameters and anisotropic temperature factors of phenakite at 1 bar are in close agreement with the previous refinements of Downs (1983). Mean cation-anion bond distances for the three symmetrically distinct tetrahedra are 1.628, 1.643, and 1.644 A, for the Si, Be1, and Be2 polyhedra, respectively (Table 6). These tetrahedra are only slightly distorted, with quadratic elongation and angle variance close to the ideal values (Table 7). Anisotropic thermal motion of the oxygens (Table 4), all of which are in planar three-coordination, may be represented by prolate spheroids, with major axes perpendicular to the cation-oxygen bonding planes.

Refined atomic positional parameters for bertrandite, with the exception of z parameters of the two berylliums and O3, are in reasonable agreement with the previous work of Solov'eva and Belov (1965). The present adjustments

Table 2. Refinement conditions and refined atomic parameters of phenakite

	1 bar	16 kbar	36 kbar	49.5 kbar
No. of Observations ($I>2\sigma$)	608	239	258	264
R (%)[b]	2.7	4.0	4.4	4.8
Weighted R (%)[b]	2.8	2.5	2.7	3.7
Extinction, r^* ($\times 10^5$)	130 (5)[a]	102 (7)	109 (7)	99 (9)

Atom	Parameter				
Si	x	0.19550 (4)	0.1947 (1)	0.1950 (2)	0.1950 (2)
	y	0.21155 (4)	0.2116 (1)	0.2118 (2)	0.2118 (1)
	z	0.74996 (6)	0.7502 (2)	0.7497 (2)	0.7496 (2)
	B	0.14 (1)	0.59 (3)	0.52 (3)	0.49 (4)
Be1	x	0.1941 (2)	0.1921 (8)	0.1944 (9)	0.1924 (8)
	y	0.2104 (2)	0.2093 (7)	0.2113 (9)	0.2096 (8)
	z	0.4155 (2)	0.4154 (6)	0.4170 (7)	0.4156 (7)
	B	0.36 (3)	0.81 (12)	0.93 (14)	0.87 (13)
Be2	x	0.1941 (2)	0.1947 (8)	0.1929 (10)	0.1932 (8)
	y	0.2118 (2)	0.2123 (7)	0.2129 (9)	0.2121 (8)
	z	0.0841 (2)	0.0820 (6)	0.0840 (8)	0.0842 (8)
	B	0.40 (3)	0.94 (12)	1.25 (14)	0.94 (13)
O1	x	0.2095 (1)	0.2098 (3)	0.2096 (4)	0.2095 (4)
	y	0.0884 (1)	0.0885 (3)	0.0885 (3)	0.0888 (3)
	z	0.7503 (1)	0.7499 (3)	0.7509 (4)	0.7508 (4)
	B	0.29 (2)	0.71 (6)	0.67 (7)	0.70 (7)
O2	x	0.3336 (1)	0.3332 (3)	0.3339 (4)	0.3334 (4)
	y	0.3332 (1)	0.3332 (3)	0.3341 (3)	0.3336 (3)
	z	0.7501 (2)	0.7493 (3)	0.7501 (3)	0.7500 (4)
	B	0.26 (2)	0.86 (5)	0.68 (6)	0.79 (6)
O3	x	0.1225 (1)	0.1227 (3)	0.1227 (3)	0.1219 (4)
	y	0.2100 (1)	0.2098 (3)	0.2101 (3)	0.2098 (3)
	z	0.9146 (1)	0.9148 (3)	0.9150 (4)	0.9151 (4)
	B	0.26 (2)	0.73 (6)	0.71 (7)	0.69 (7)
O4	x	0.1225 (1)	0.1212 (3)	0.1218 (4)	0.1224 (4)
	y	0.2090 (1)	0.2090 (3)	0.2086 (3)	0.2094 (4)
	z	0.5850 (1)	0.5849 (3)	0.5851 (4)	0.5840 (4)
	B	0.28 (2)	0.77 (7)	0.85 (8)	0.68 (7)

[a] Parenthesized figures represent *esd*'s.

[b] $R=\sum[|F_o|-|F_c|]/\sum F_o$
Weighted $R=[\sum w(|F_o|-|F_c|)^2/\sum w F_o^2]^{1/2}$

to z parameters lead to reasonable Be–O distances, as opposed to the untenable values (as long as 1.78 A) in the previous work. Mean T–O distances for the Si, Be1, and Be2 tetrahedra are 1.619, 1.641, and 1.641 A, respectively (Table 8). As in phenakite, these corner-linked tetrahedra are relatively undistorted. Anisotropic thermal parameters (Table 5) have not been reported previously for bertrandite. The three oxygens, in planar three-coordination, O1, O2 and O3, have thermal motion that may be represented by a prolate ellipsoid with major axis perpendicular to the plane of cation-anion bonding. The magnitude of the major axis is approximately twice that of the other two axes in these anions. The O4, OH1, and OH2 anions are two-coordinated, and have minimum thermal motion approximately parallel to the T–O–T bonding direction.

Unit-Cell Compressibilities and Bulk Moduli

Linear compressibilities and pressure-volume equation-of-state parameters have been calculated from unit-cell data in Table 1. Unit-cell edges may be expressed as functions of pressure:

$$a=a_0-d_1 P+d_2 P^2.$$

Cell-edge compressibilities of phenakite and bertrandite are approximately linear with pressure, so that only the d_1 terms are required:

For phenakite:

$$a=12.468\pm0.002-(0.00200\pm0.00004)P$$
$$(\beta_\perp=1.60\pm0.03\times10^{-4}\ \text{kbar}^{-1})$$

$$c=\ 8.248\pm0.002-(0.00119\pm0.00007)P$$
$$(\beta_\parallel=1.45\pm0.07\times10^{-4}\ \text{kbar}^{-1})$$

For bertrandite:

$$a=\ 8.714\pm0.001-(0.00315\pm0.00007)P$$
$$(\beta_a=3.61\pm0.08\times10^{-4}\ \text{kbar}^{-1})$$

$$b=15.266\pm0.004-(0.0088\pm0.0002)P$$
$$(\beta_b=5.78\pm0.13\times10^{-4}\ \text{kbar}^{-1})$$

Table 3. Refinement conditions and refined atomic parameters of bertrandite

	1 bar	23 kbar	41 kbar
No of observations ($I>2\sigma$)	446	143	143
R (%)[b]	3.7	3.5	3.1
weighted R (%)[b]	3.8	4.1	3.5
Extinction, r^* ($\times 10^6$)	3 (3)[a]	3 (4)	8 (4)

Atom	Parameter			
Si	x	0.3254 (1)	0.3261 (3)	0.3270 (2)
	y	0.1144 (1)	0.1135 (1)	0.1128 (1)
	z	0.6523 (17)	0.6546 (46)	0.6499 (66)
	B	0.21 (2)	0.52 (5)	0.45 (4)
Be1	x	0.1735 (8)	0.1679 (14)	0.1723 (15)
	y	0.0527 (3)	0.0536 (6)	0.0545 (6)
	z	0.1628 (48)	0.094 (22)	0.136 (30)
	B	0.45 (10)	0.6 (3)	0.8 (2)
Be2	x	0.3264 (7)	0.3246 (17)	0.3297 (15)
	y	0.2203 (3)	0.2214 (7)	0.2233 (7)
	z	0.1517 (51)	0.061 (17)	0.065 (22)
	B	0.48 (7)	0.6 (3)	0.5 (3)
O1	x	0.2897 (3)	0.2939 (6)	0.2956 (5)
	y	0.1244 (2)	0.1246 (3)	0.1233 (3)
	z	0[c]	0[c]	0[c]
	B	0.38 (4)	0.8 (4)	0.8 (4)
O2	x	0.2101 (4)	0.2967 (8)	0.2048 (6)
	y	0.0431 (2)	0.0438 (3)	0.0443 (3)
	z	0.5074 (8)	0.4987 (72)	0.5034 (67)
	B	0.31 (5)	1.0 (2)	0.8 (1)
O3	x	0.2934 (4)	0.2948 (8)	0.2990 (8)
	y	0.2093 (2)	0.2081 (4)	0.2986 (4)
	z	0.5024 (8)	0.4904 (83)	0.4846 (88)
	B	0.42 (5)	0.9 (2)	1.1 (2)
O4	x	0	0	0
	y	0.5852 (2)	0.5821 (4)	0.5796 (4)
	z	0.5951 (11)	0.5843 (92)	0.5880 (94)
	B	0.46 (8)	0.9 (2)	0.7 (2)
OH1	x	0	0	0
	y	0.7553 (2)	0.7600 (5)	0.7628 (4)
	z	0.0886 (10)	0.0826 (96)	0.0533 (93)
	B	0.54 (9)	0.87 (2)	0.5 (2)
OH2	x	0	0	0
	y	0.0872 (2)	0.0916 (4)	0.0947 (4)
	z	0.0993 (11)	0.0760(101)	0.0762(100)
	B	0.53 (9)	0.6 (2)	0.6 (2)

[a] Parenthesized figures represent *esd*'s
[b] $R=\sum[|F_o|-|F_c|]/\sum F_o$
weighted $R=[\sum w(|F_o|-|F_c|)^2/\sum w F_o^2]^{1/2}$
[c] The Z parameter of O1 is arbitrarily chosen to be 0 in conformity with previous authors

$$c = 4.567 \pm 0.001 - (0.00146 \pm 0.00005)P$$
$$(\beta_c = 3.19 \pm 0.10 \times 10^{-4}\ \text{kbar}^{-1})$$

The compressibility of phenakite is nearly isotropic, with the a axis approximately 10 percent more compressible than c. Bertrandite compression, on the other hand, is very anisotropic, with compression ratios of $a:b:c = 1.13:1.81:1.00$.

The bulk modulus, K_0, and its pressure derivative, K', were calculated from pressure-volume data by least-squares procedures. Bulk moduli of the two orthosilicates were initially calculated with a first-order Birch-Murnaghan equation of state based on the assumption that $K'=4$ (Hazen and Finger 1982). Resultant bulk moduli are 1.98 ± 0.05 and 0.72 ± 0.02 Mbar for phenakite and bertrandite, respectively. Alternatively, a second-order Birch-Murnaghan equation of state may be employed to calculate both K and K' from the pressure-volume data. Phenakite parameters are $K=2.01 \pm 0.08$ Mbar and $K'=2 \pm 4$, in agreement with the 2.1-Mbar bulk modulus determined by Yeganeh-Haeri and Weidner (in preparation). Second-order parameters for bertrandite are $K=0.70 \pm 0.03$ Mbar and $K'=5.3 \pm 1.5$.

High-Pressure Crystal Structure of Phenakite

Each of phenakite's three symmetrically distinct cations, two berylliums and one silicon, is surrounded by a tetrahedron of oxygens, whereas each of the four symmetrically distinct oxygens in the structure is coordinated to a quasi-planar triad of one silicon and two berylliums. These structural units form a three-dimensional framework of corner-linked tetrahedra (Fig. 1). Four- and six-member rings of tetrahedra occur in alternation in the (001) plane, whereas three-member rings are found perpendicular to this plane. The structure may also be visualized in terms of its distinctive chains of tetrahedra parallel to the c axis with the regular pattern Be–Be–Si–Be–Be–Si–.... The pressure response of the phenakite structure may be described in terms of changes both in the three distinct cation polyhedra and in angles between these polyhedra. Selected interatomic distances and angles for phenakite at several pressures are recorded in Table 6.

All three tetrahedra in the phenakite structure undergo significant compression. Tetrahedral bulk moduli may be calculated on the basis of changes in the volume of enclosure defined by positions of the four coordinating oxygens. For Be1, Be2 and Si tetrahedra these values are 2.3 ± 0.3, 1.7 ± 0.3 and 2.7 ± 0.4 Mbar, respectively (Table 7). Polyhedral distortions, as measured by quadratic elongation and angle variance (Hazen and Finger 1982) do not vary significantly with pressure, so compression, rather than distortion, is the principal polyhedral response to pressure.

Compression in solids comprised of cation polyhedra occur by a combination of polyhedral compression and changes in interpolyhedral angles (Hazen and Finger 1985). In phenakite these $T-O-T$ angles (Table 6) are all close to 120° and are all unchanged within one estimated standard deviation between room pressure and 50 kbar. Bond-angle bending is thus not a factor in phenakite compression. The slight anisotropy of phenakite compression, with c about 10 percent less compressible than a, may be a consequence of the short metal-metal separations parallel to c.

High-Pressure Crystal Structure of Bertrandite

Bertrandite differs from phenakite in composition only by the substitution of two hydroxyls for one oxygen. This small compositional change, however, results in important differences in atomic topology. Bertrandite has three symmetrically distinct cation tetrahedra: silicon surrounded by four oxygens, and two symmetrically distinct berylliums, each surrounded by three oxygens and one hydroxyl. Of four

Table 4. Anisotropic temperature parameters of phenakite at room pressure

Atom	Parameter	$\beta \times 10^4$	Axis	rms (Å) Displacement	Angle with respect to:		
					a	b	c
Si	β_{11}	3.2 (4)[a]	r_1	0.036 (3)	98 (28)	94 (18)	13 (17)
	β_{22}	4.0 (4)	r_2	0.040 (3)	168 (23)	51 (0)	97 (26)
	β_{33}	3.9 (6)	r_3	0.049 (3)	83 (0)	39 (0)	79 (9)
	β_{12}	2.1 (3)					
	β_{13}	0.4 (4)					
	β_{23}	0.5 (4)					
Be1	β_{11}	9.5 (15)	r_1	0.055 (8)	73 (16)	109 (22)	21 (19)
	β_{22}	8.3 (16)	r_2	0.070 (6)	82 (51)	154 (40)	104 (26)
	β_{33}	9.7 (27)	r_3	0.076 (6)	19 (27)	107 (50)	105 (20)
	β_{12}	4.5 (14)					
	β_{13}	−1.1 (17)					
	β_{23}	0.7 (17)					
Be2	β_{11}	8.9 (16)	r_1	0.063 (8)	100 (50)	82 (31)	11 (48)
	β_{22}	10.7 (16)	r_2	0.069 (7)	169 (48)	57 (25)	100 (50)
	β_{33}	11.7 (27)	r_3	0.079 (6)	86 (24)	34 (23)	93 (20)
	β_{12}	5.5 (15)					
	β_{13}	0.1 (18)					
	β_{23}	−0.3 (18)					
O1	β_{11}	9.9 (9)	r_1	0.0468 (6)	118 (7)	25 (25)	115 (25)
	β_{22}	5.4 (9)	r_2	0.0557 (5)	82 (14)	115 (26)	153 (25)
	β_{33}	8.6 (16)	r_3	0.0767 (3)	29 (7)	91 (7)	96 (8)
	β_{12}	4.9 (8)					
	β_{13}	−0.7 (9)					
	β_{23}	0.4 (9)					
O2	β_{11}	4.8 (9)	r_1	0.053 (5)	34 (56)	88 (52)	77 (28)
	β_{22}	5.4 (9)	r_2	0.056 (5)	56 (56)	159 (30)	110 (26)
	β_{33}	10.9 (16)	r_3	0.063 (4)	90 (22)	110 (28)	24 (27)
	β_{12}	2.5 (7)					
	β_{13}	−0.5 (9)					
	β_{23}	−0.8 (9)					
O3	β_{11}	6.1 (9)	r_1	0.045 (6)	106 (32)	83 (20)	16 (32)
	β_{22}	8.9 (9)	r_2	0.052 (5)	162 (30)	54 (10)	106 (33)
	β_{33}	5.9 (15)	r_3	0.073 (4)	83 (9)	37 (9)	86 (8)
	β_{12}	4.9 (7)					
	β_{13}	0.6 (9)					
	β_{23}	0.4 (10)					
O4	β_{11}	5.4 (9)	r_1	0.044 (5)	84 (33)	96 (15)	7 (27)
	β_{22}	9.9 (10)	r_2	0.051 (5)	172 (25)	66 (8)	85 (33)
	β_{33}	5.7 (16)	r_3	0.077 (4)	95 (7)	25 (7)	86 (6)
	β_{12}	4.5 (8)					
	β_{13}	0.1 (9)					
	β_{23}	0.6 (9)					

[a] Parenthesized figures represent *esd*'s

symmetrically independent oxygens, three have the three-coordinated quasi-planar configuration of two berylliums and one silicon observed in phenakite. The fourth oxygen, O4, bridges two silicons to form a diorthosilicate Si_2O_7 group. The two symmetrically independent hydroxyls play a structural role similar to that of O4 by bridging pairs of beryllium tetrahedra to form Be_2O_7 groups. The structure may be constructed from (001) sheets of tetrahedra that form interconnected six-member rings, identical in polyhedral topology to the tetrahedral layers of sheet silicates. A projection of the bertrandite structure is given in Figure 2, and selected distances and angles are listed in Table 8.

Polyhedral bulk moduli for Be1, Be2 and Si tetrahedra are 2.1 ± 0.4, 1.4 ± 0.7 and 1.8 ± 0.5 Mbar, respectively. All three polyhedra thus undergo significant compression between 1 bar and 41 kbar. Note, however, that the average polyhedral bulk modulus of about 2 Mbar is significantly greater than the 0.7-Mbar macroscopic modulus of bertrandite. Bending of $T-O-T$ angles thus appears to be the dominant mechanism of bertrandite compression.

Precise values for $T-O-T$ angles are not available for high-pressure structures of bertrandite. Beryllium has fewer than four electrons associated with each nucleus in oxides and silicates, so it is difficult to locate Be positions with precision in a high-pressure X-ray experiment. Uncertainties in Be positions, in turn, lead to large uncertainties in $T-O-T$ angles. Nevertheless, significant changes in several angles (Si−O4−Si, Be1−O1−Be2 and Be2−O3−Be2,

Table 5. Anisotropic temperature parameters of bertrandite at room pressure

Atom	Parameter	$\beta \times 10^4$	Axis	rms (Å) Displacement	Angle with respect to:		
					a	b	c
Si	β_{11}	9.5 (10)[a]	r_1	0.02 (3)	110 (16)	67 (14)	31 (11)
	β_{22}	2.6 (3)	r_2	0.06 (1)	95 (76)	27 (42)	116 (27)
	β_{33}	11 (4)	r_3	0.06 (1)	21 (14)	77 (70)	74 (49)
	β_{12}	0.8 (6)					
	β_{13}	5 (7)					
	β_{23}	−2 (3)					
Be1	β_{11}	24 (5)	r_1	Non-positive definite			
	β_{22}	5 (1)	r_2				
	β_{33}	20 (31)	r_3				
	β_{12}	−0.5 (25)					
	β_{13}	45 (23)					
	β_{23}	5 (10)					
Be2	β_{11}	15 (5)	r_1	Non-positive definite			
	β_{22}	5 (1)	r_2				
	β_{33}	58 (20)	r_3				
	β_{12}	3 (3)					
	β_{13}	42 (33)					
	β_{23}	−24 (18)					
O1	β_{11}	25 (4)	r_1	0.04 (1)	91 (12)	111 (45)	21 (46)
	β_{22}	3 (1)	r_2	0.05 (1)	102 (8)	156 (41)	111 (46)
	β_{33}	18 (11)	r_3	0.10 (1)	12 (8)	101 (8)	94 (7)
	β_{12}	−2 (2)					
	β_{13}	−2 (5)					
	β_{23}	1 (3)					
O2	β_{11}	16 (4)	r_1	0.04 (2)	71 (12)	99 (22)	21 (13)
	β_{22}	3 (1)	r_2	0.06 (1)	100 (17)	168 (20)	96 (21)
	β_{33}	19 (13)	r_3	0.08 (1)	22 (13)	97 (16)	110 (12)
	β_{12}	−0 (1)					
	β_{13}	−9 (6)					
	β_{23}	1 (3)					
O3	β_{11}	27 (4)	r_1	0.04 (2)	91 (12)	83 (27)	7 (28)
	β_{22}	3 (1)	r_2	0.06 (1)	72 (7)	161 (12)	83 (29)
	β_{33}	14 (12)	r_3	0.11 (1)	18 (7)	72 (7)	91 (8)
	β_{12}	3 (1)					
	β_{13}	−0 (6)					
	β_{23}	−1 (3)					
O4[b]	β_{11}	8 (5)	r_1	0.05 (2)	0	90	90
	β_{22}	5 (1)	r_2	0.07 (1)	90	151 (20)	119 (20)
	β_{33}	80 (30)	r_3	0.10 (1)	90	119 (20)	29 (20)
	β_{23}	−5 (4)					
OH1[b]	β_{11}	13 (5)	r_1	0.07 (2)	90	127 (15)	37 (15)
	β_{22}	7 (1)	r_2	0.07 (1)	0	90	90
	β_{33}	66 (27)	r_3	0.10 (1)	90	37 (15)	53 (15)
	β_{23}	9 (4)					
OH2[b]	β_{11}	17 (5)	r_1	0.05 (2)	90	113 (12)	23 (12)
	β_{22}	8 (1)	r_2	0.08 (1)	0	90	90
	β_{33}	39 (28)	r_3	0.10 (1)	90	23 (13)	67 (13)
	β_{23}	8 (4)					

[a] Parenthesized figures represent *esd*'s
[b] $\beta_{12}=\beta_{13}=0$

for example) point to the importance of angle bending in bertrandite compression.

Discussion

Polyhedral Bulk Moduli

Hazen and Finger (1979, 1982) proposed that each type of cation polyhedron has its own characteristic compressibility, independent of the structure in which it is found. This relationship has been demonstrated for several octahedrally coordinated cations, but smaller cations in tetrahedral coordination have not been adequately tested. Errors associated with polyhedral volumes of small, incompressible polyhedra are comparable to the observed changes in volume with pressure, so precise tetrahedral bulk moduli cannot usually be calculated. The present data on beryllium silicates, which are improved compared with previous high-pressure, X-ray

Table 6. Selected bond distances and angles of phenakite

Bond/Angle	1 bar	16 kbar	36 kbar	49.5 kbar
Si Tetrahedron				
Si–O1	1.627 (1)[a]	1.633 (3)	1.625 (4)	1.619 (4)
Si–O2	1.626 (1)	1.628 (4)	1.629 (4)	1.618 (4)
Si–O3	1.629 (1)	1.618 (3)	1.620 (4)	1.622 (4)
Si–O4	*1.628 (1)*	*1.630 (3)*	*1.616 (4)*	*1.619 (4)*
Mean Si–O	1.628	1.627	1.623	1.620
O1–Si–O2	108.4 (1)	107.9 (2)	108.2 (2)	108.2 (2)
O1–Si–O3	108.0 (1)	108.1 (2)	107.7 (2)	107.7 (2)
O1–Si–O4	107.8 (1)	107.8 (2)	107.9 (2)	108.0 (2)
O2–Si–O3	109.5 (1)	109.8 (2)	109.3 (2)	109.6 (2)
O2–Si–O4	109.8 (1)	109.7 (2)	110.1 (2)	109.8 (2)
O3–Si–O4	113.2 (1)	113.4 (2)	113.5 (2)	113.5 (2)
Be1 Tetrahedron				
Be1–O1	1.639 (2)	1.622 (6)	1.644 (8)	1.625 (8)
Be1–O2	1.638 (3)	1.661 (9)	1.626 (11)	1.648 (10)
Be1–O4	1.654 (2)	1.649 (7)	1.638 (7)	1.631 (9)
Be1–O4	*1.642 (3)*	*1.627 (8)*	*1.638 (10)*	*1.628 (8)*
Mean Be1–O	1.643	1.640	1.637	1.633
O1–Be1–O2	109.5 (1)	108.8 (4)	109.6 (5)	109.3 (5)
O1–Be1–O4	108.3 (1)	108.9 (4)	107.4 (5)	108.9 (5)
O1–Be1–O4	114.3 (1)	114.8 (5)	114.2 (5)	114.9 (5)
O2–Be1–O4	108.3 (1)	107.2 (5)	108.0 (6)	107.1 (5)
O2–Be1–O4	108.4 (1)	108.4 (4)	109.7 (5)	108.2 (5)
O4–Be1–O4	107.8 (1)	108.4 (4)	107.9 (5)	108.2 (5)
Be2 Tetrahedron				
Be2–O1	1.633 (2)	1.649 (7)	1.610 (9)	1.613 (8)
Be2–O2	1.637 (3)	1.627 (9)	1.624 (10)	1.626 (9)
Be2–O3	1.655 (3)	1.659 (8)	1.673 (9)	1.648 (9)
Be2–O3	*1.652 (2)*	*1.633 (6)*	*1.628 (8)*	*1.635 (8)*
Mean Be2–O	1.644	1.642	1.634	1.630
O1–Be2–O2	109.9 (1)	109.6 (4)	110.4 (5)	110.3 (5)
O1–Be2–O3	107.7 (1)	106.9 (4)	107.3 (5)	107.8 (5)
O1–Be2–O3	114.6 (1)	114.4 (5)	115.7 (6)	114.8 (6)
O2–Be2–O3	107.5 (1)	107.6 (5)	106.3 (6)	106.7 (5)
O2–Be2–O3	108.9 (1)	109.8 (4)	109.3 (5)	109.2 (5)
O2–Be2–O3	107.9 (1)	108.3 (4)	107.4 (5)	107.7 (5)
O1 (3-coordinated)				
O1–Si	1.627 (1)	1.633 (3)	1.625 (4)	1.619 (4)
O1–Be1	1.639 (2)	1.622 (7)	1.644 (8)	1.625 (3)
O1–Be2	1.633 (2)	1.648 (7)	1.610 (9)	1.613 (8)
Si–O1–Be1	123.2 (1)	122.9 (3)	122.7 (4)	122.5 (4)
Si–O1–Be2	123.2 (1)	122.8 (3)	123.0 (4)	123.4 (4)
Be1–O1–Be2	113.4 (1)	114.0 (3)	114.2 (4)	113.9 (4)
O2 (3-coordinated)				
O2–Si	1.626 (1)	1.628 (4)	1.629 (4)	1.618 (4)
O2–Be1	1.636 (3)	1.661 (9)	1.626 (10)	1.648 (10)
O2–Be2	1.637 (2)	1.627 (9)	1.624 (11)	1.626 (9)
Si–O2–Be1	120.2 (1)	120.0 (3)	119.6 (4)	119.8 (4)
Si–O2–Be2	120.3 (1)	120.4 (4)	121.1 (5)	120.8 (4)
Bel–O2–Be2	119.5 (1)	119.7 (5)	119.3 (6)	119.4 (5)
O3 (3-coordinated)				
O3–Si	1.629 (1)	1.618 (3)	1.620 (4)	1.622 (4)
O3–Be2	1.652 (2)	1.633 (6)	1.628 (8)	1.635 (8)
O3–Be2	1.655 (3)	1.659 (8)	1.673 (9)	1.648 (8)
Si–O3–Be2	114.3 (1)	114.2 (3)	115.3 (4)	114.5 (4)
Si–O3–Be2	123.7 (1)	124.0 (3)	123.3 (4)	123.5 (3)
Be2–O3–Be2	121.7 (1)	121.6 (3)	121.2 (4)	121.8 (4)
O4 (3-coordinated)				
O4–Si	1.628 (1)	1.630 (3)	1.616 (4)	1.619 (4)
O4–Be1	1.654 (2)	1.649 (7)	1.638 (7)	1.628 (8)
O4–Be1	1.642 (2)	1.627 (8)	1.638 (9)	1.631 (8)
Si–O4–Be1	114.5 (1)	114.3 (3)	114.0 (4)	114.8 (4)
Si–O4–Be1	123.3 (1)	123.4 (3)	123.9 (3)	122.9 (3)
Be1–O4–Be1	122.0 (1)	121.9 (3)	122.0 (4)	122.0 (4)

[a] Parenthesized figures represent *esd*'s

Table 7. Polyhedral volumes and distortion parameters of phenakite and bertrandite at several pressures

Atom Parameter	1 bar	16 kbar	36 kbar	49.5 kbar
A. Phenakite				
Si Vol (Å^3)	2.218 (2)[a]	2.207 (7)	2.190 (8)	2.177 (9)
QE[b]	1.001 (1)	1.001 (4)	1.001 (4)	1.001 (5)
AV[c]	4.1	4.7	5.1	4.9
Be1 Vol (Å^3)	2.279 (4)	2.257 (13)	2.246 (15)	2.230 (15)
QE	1.001 (2)	1.002 (8)	1.002 (9)	1.002 (9)
AV	6.0	7.5	6.6	7.9
Be2 Vol (Å^3)	2.284 (4)	2.265 (13)	2.231 (15)	2.218 (14)
QE	1.002 (2)	1.002 (7)	1.003 (9)	1.002 (8)
AV	7.2	7.3	11.8	8.7

Atom Parameter	1 bar	23 kbar	41 kbar
B. Bertrandite			
Si Vol (Å^3)	2.182 (6)	2.16 (2)	2.13 (2)
QE	1.001 (6)	1.00 (2)	1.00 (2)
AV	2	8	4
Be1[d] Vol (Å^3)	2.256 (7)	2.23 (4)	2.21 (4)
Be2[d] Vol (Å^3)	2.261 (7)	2.20 (4)	2.20 (4)

[a] Parenthesized figures represent *esd*'s

[b] QE = quadratic elongation = $\sum_{i=1}^{n} [(1_i/1_0)^2/n]$ (Robinson et al., 1971)

[c] AV = angle variance = $\sum_{i=1}^{n} [(\theta_i - \theta_0)^2/(n-1)]$ (Robinson et al., 1971)

[d] Beryllium positions in bertrandite are too poorly constrained to calculate meaningful distortion parameters.

measurements because of unusually long counting times and reduced peak-to-background ratio, result in more precise determination of tetrahedral bulk moduli.

Polyhedral bulk moduli for the four symmetrically distinct Be tetrahedra in these two beryllium minerals are 2.3 ± 0.3 and 1.7 ± 0.3 Mbar for phenakite and 1.4 ± 0.7 and 1.8 ± 0.5 Mbar for bertrandite. All these values are consistent with 2 Mbar, which is also the observed bulk modulus of beryllium tetrahedra in the oxide, bromellite (Hazen and Au, in preparation). Data from these beryllium minerals are thus consistent with the hypothesis that the bulk moduli of beryllium tetrahedra are invariant in different structures. Note, however, that the observed 2-Mbar tetrahedral bulk modulus is significantly greater than the 1.5-Mbar value predicted by the empirical relationship of Hazen and Finger (1979, 1982). High-pressure crystallographic studies of beryl, chrysoberyl and euclase, now in progress, will provide additional values for beryllium polyhedral compression.

The bulk moduli of silicon tetrahedra in phenakite and bertrandite are 2.7 ± 0.4 and 1.8 ± 0.5 Mbar, respectively. Compressibilities of silicon tetrahedra in phenakite and bertrandite, therefore, are similar to those of beryllium tetrahedra. Silicon values are significantly less than the 4 Mbar or greater modulus predicted by Hazen and Finger (1979) and the modulus of approximately 4 Mbar observed in silica polymorphs by Jorgensen (1978), Levien et al. (1980) and Levien and Prewitt (1981). It is evident, therefore, that the bulk modulus of silicon tetrahedra is probably not independent of crystal structure. Although more data are required, preliminary analysis of a number of high-pressure silicates suggests that the bulk modulus of silicon tetrahedra may be correlated with the number of Si–O–Si bond angles that are free to bend. In quartz and coesite, where all Si–O–Si bonds bend with increasing pressure, the tetrahedral bulk modulus is relatively large. Most of the compressive force is applied to bond bending rather than bond shortening. In phenakite and bertrandite, on the other hand, the bending of Si–O–Si angles is more restricted. Compressive force is applied primarily to bond shortening as opposed to bond bending. Thus, the compressibility of silicon tetrahedra may vary according to the "stiffness" of the structural units that surround them. In quartz the weak Si–O–Si bonds result in little tetrahedral compression, whereas in phenakite the more rigid Be–Si tetrahedral framework leads to significantly greater compression of silicon tetrahedra.

Compression Anisotropies

Linear compressibilities in phenakite and bertrandite differ by a factor of four. These differences are directly related to the degree of $T-O-T$ bond-angle bending that occurs. The least compressible direction is parallel to the c axis of phenakite, along which chains composed of rigid, three-member rings of beryllium and silicon tetrahedra are unable to bend (Fig. 1-B). The observed $\beta_{\|} = 1.45 \times 10^{-4}$ kbar^{-1} is equivalent to the linear compressibility of the constituent polyhedra. The compressibility of phenakite perpendicular to c is only slightly greater and is constrained by the restrictions imposed by hexagonal symmetry on $T-O-T$ bending in the six-member rings (Fig. 1-A).

The most compressible direction in either of these two minerals is parallel to the b axis of bertrandite, corresponding to the direction in which 6-member tetrahedral rings are most easily deformed (Fig. 2). Small changes in $T-O-T$ angles within these rings lead to a large change in the b dimension, just as polyhedral rotation in the layer silicates results in conformation of tetrahedral layers to octahedral layers of different sizes (Hazen and Finger 1985). Bertrandite compression perpendicular to these layers, however, is controlled predominantly by three- and four-member rings, which are significantly less deformable than the larger rings.

Compression Mechanisms

High-pressure crystal structures of phenakite and bertrandite reveal two different compression mechanisms in the beryllium silicates. The first mechanism, metal-oxygen bond compression in beryllium and silicon tetrahedra, results in bulk moduli of approximately 2 Mbar for all polyhedra in both structures. The 2-Mbar crystal bulk modulus of phenakite is a consequence of this polyhedral value.

The second mechanism, bending of angles between corner-linked tetrahedra, occurs only in bertrandite and results in the significantly greater compressibility of that mineral. In spite of the fact that all tetrahedra in phenakite and bertrandite are corner-linked, only a few of the many different $T-O-T$ angles are observed to change significantly with increasing pressure. Two factors, symmetry and distribution of three member rings, are observed to limit bending of some $T-O-T$ angles. Bond bending may be

Table 8. Selected bond distances and angles of bertrandite

Bertrandite

Bond/Angle	1 bar		23 kbar		41 kbar	
Si Tetrahedron						
Si–O1	1.626	(8)[a]	1.599	(21)	1.610	(29)
Si–O2	1.625	(4)	1.633	(15)	1.606	(14)
Si–O3	1.617	(4)	1.628	(15)	1.629	(18)
Si–O4	*1.607*	*(2)*	*1.607*	*(7)*	*1.590*	*(9)*
Mean Si–O	1.619		1.617		1.609	
O1–Si–O2	110.1	(3)	112	(1)	111	(1)
O1–Si–O3	107.2	(3)	109	(1)	110	(1)
O1–Si–O4	111.5	(4)	113	(2)	111	(2)
O2–Si–O3	108.6	(3)	105	(1)	106	(1)
O2–Si–O4	109.5	(3)	108	(1)	110	(1)
O3–Si–O4	110.0	(3)	109	(1)	109	(1)
Be1 Tetrahedron						
Be1–O1	1.666	(9)	1.58	(3)	1.60	(5)
Be1–O2	1.656	(22)	1.87	(8)	1.69	(13)
Be1–O2	1.612	(10)	1.56	(2)	1.61	(5)
Be1–OH2	*1.629*	*(9)*	*1.56*	*(2)*	*1.62*	*(3)*
Mean Be1–O	1.641		1.64		1.63	
O1–Be1–O2	112.1	(8)	114	(3)	109	(4)
O1–Be1–O2	105.8	(8)	101	(3)	109	(5)
O1–Be1–OH2	105.8	(7)	112	(2)	108	(4)
O2–Be1–O2	107.4	(7)	99	(3)	105	(4)
O2–Be1–OH2	112.8	(9)	104	(4)	110	(6)
O2–Be1–OH2	112.9	(9)	122	(2)	116	(4)
Be2 Tetrahedron						
Be2–O1	1.650	(9)	1.51	(2)	1.55	(2)
Be2–O3	1.647	(23)	1.98	(5)	1.92	(7)
Be2–O3	1.639	(12)	1.51	(2)	1.54	(2)
Be2–OH1	*1.628*	*(7)*	*1.63*	*(1)*	*1.58*	*(2)*
Mean Be2–O	1.641		1.66		1.65	
O1–Be2–O3	106.6	(7)	93	(3)	93	(4)
O1–Be2–O3	106.4	(9)	121	(2)	117	(2)
O1–Be2–OH1	113.4	(7)	121	(1)	122	(1)
O3–Be2–O3	111.2	(7)	101	(2)	102	(3)
O3–Be2–OH1	111.7	(10)	113	(1)	102	(4)
O3–Be2–OH1	107.5	(8)	96	(3)	114	(2)
O1 (3-coordinated)						
O1–Si	1.626	(8)	1.60	(2)	1.61	(3)
O1–Be1	1.666	(9)	1.58	(3)	1.59	(5)
O1–Be2	1.651	(9)	1.51	(3)	1.55	(2)
Si–O1–Be1	120.9	(10)	136	(3)	132	(4)
Si–O1–Be2	119.4	(7)	108	(4)	115	(4)
Be1–O1–Be2	117.2	(7)	104	(3)	104	(4)
O2 (3-coordinated)						
O2–Si	1.623	(4)	1.63	(2)	1.61	(1)
O2–Be1	1.613	(22)	1.56	(2)	1.61	(5)
O2–Be1	1.656	(10)	1.87	(8)	1.69	(1)
Si–O2–Be1	117.3	(4)	119	(1)	117	(1)
Si–O2–Be1	122.5	(6)	128	(2)	123	(3)
Be1–O2–Be1	117.4	(8)	108	(3)	115	(5)
O3 (3-coordinated)						
O3–Si	1.627	(4)	1.628	(15)	1.629	(18)
O3–Be2	1.636	(23)	1.97	(5)	1.92	(7)
O3–Be2	1.647	(12)	1.51	(2)	1.54	(2)
Si–O3–Be2	118.3	(4)	121.2	(10)	122.0	(1)
Si–O3–Be2	121.1	(5)	129.0	(5)	125.1	(7)
O3 (3-coordinated)						
Be2–O3–Be2	116.7	(8)	103.0	(19)	104.7	(25)
O4 (2-coordinated)						
O4–Si [2][b]	1.606	(2)	1.607	(9)	1.590	(9)
Si–O4–Si	142.5	(4)	138.4	(16)	138.1	(17)
OH1 (2-coordinated)						
OH1–Be2 [2]	1.630	(7)	1.626	(14)	1.578	(15)
Be2–OH1–Be2	136.2	(9)	137.5	(10)	136.0	(10)
OH2 (2-coordinated)						
OH2–Be1 [2]	1.627	(9)	1.561	(15)	1.620	(28)
Be1–OH2–Be1	136.6	(7)	136.5	(13)	132	(4)

[a] Parenthesized fiugres represent *esd*'s

[b] Bracketed figures represent bond multiplicities

restricted, in a sense, by the presence of symmetry elements, such as the six-fold rotation axis associated with hexagonal phenakite's six-member rings. The energy required to change symmetry (i.e., a phase transition) is greater than the energy required to undergo compression without such a modification of symmetry. Ditrigonal rotation, as observed in many layer silicates, is not consistent with phenakite's hexagonal symmetry, so that distortion of the rings is not energetically favorable. Similar $T-O-T$ bending restrictions must limit compressibility of the high-temperature (i.e., high-symmetry) forms of quartz, tridymite, cristobalite and other tetrahedral framework structures. Three-member rings of tetrahedra impose additional limitations on $T-O-T$ bending. Structural directions parallel to chains of three-member rings (as in phenakite parallel to the c axis) or sheets of these rings (as in bertrandite parallel to the c axis), therefore, have relatively low compressibilities.

Summary

High-pressure structure variations of phenakite and bertrandite are a consequence of bond compression in all beryllium and silicon tetrahedra, as well as the bending of selected $T-O-T$ angles. The phenakite structure has both topological and symmetrical limitations on intertetrahedral bending, so that compressibility is nearly isotropic and is similar in magnitude to that of the constituent cation polyhedra. The bertrandite structure, which may undergo some $T-O-T$ bending in the $a-b$ plane, displays anisotropic compression and a significantly greater bulk compressibility than that of the constituent polyhedra. High-pressure studies now in progress on other beryllium minerals should further elucidate the relationships between the structure, compressibility and elasticity of minerals.

Acknowledgments. The authors gratefully acknowledge the constructive reviews of J.W. Downs, D.J. Weidner, T. Yamanaka, A. Yeganeh-Haeri and H.S. Yoder, Jr. This research was supported by National Science Foundation grants EAR83–19209 and EAR84–19982.

PHENAKITE Be_2SiO_4

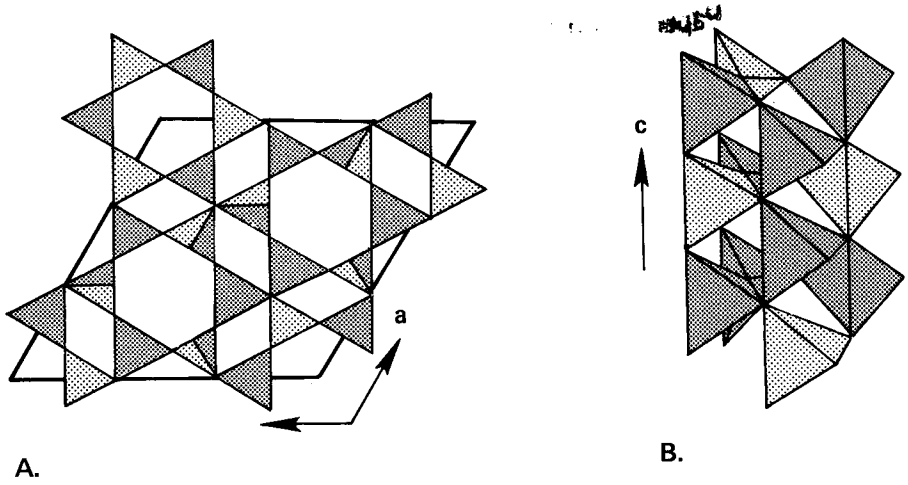

Fig. 1 A, B. The structure of phenakite: (**A**) *c*-axis projection showing six- and four-member tetrahedral rings. Shaded and unshaded tetrahedra represent silicon and beryllium, respectively. Half-shaded tetrahedra represent superposition of a silicon and a beryllium tetrahedron parallel to the *c* axis. (**B**) View showing chains of tetrahedra perpendicular to the *c* axis. Note the three-member tetrahedral rings, which act as relatively rigid structural units

BERTRANDITE $Be_4[Si_2O_7]\ (OH)_2$

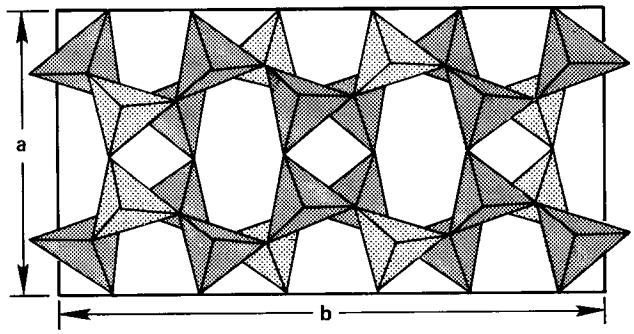

Fig. 2. The structure of bertrandite in *c*-axis projection (after Solov'eva and Belov 1965). Shaded tetrahedra represent silicon; unshaded tetrahedra represent beryllium. Sheets of interconnected six-member rings lie in the $a-b$ plane. These planes are joined along the *c* axis by three- and four-member rings

References

Barton MD (1986) Phase equilibria and thermodynamic properties of minerals in the $BeO-Al_2O_3-SiO_2-H_2O$ (BASH) system, with petrologic applications. Am Mineral 71:in press

Downs JW (1983) An experimental examination of the electron distribution in bromellite, BeO, and phenacite, Be_2SiO_4. PhD Thesis, Virginia Polytechnic Institute and State University, Blacksburg, Virginia

Hamilton WC (1974) Angle settings for four-circle diffractometers. In: International Tables for X-ray Crystallography, Vol 4. Kynoch Press, Birmingham, England, pp 273–284

Hazen RM (1985) Comparative crystal chemistry and the polyhedral approach. Rev Mineral 14:317–346

Hazen RM, Finger LW (1979) Bulk modulus-volume relationship for cation-anion polyhedra. J Geophys Res 84:6723–6728

Hazen RM, Finger LW (1982) Comparative Crystal Chemistry. Wiley, New York

Hazen RM, Finger LW (1985) Crystals at high pressure. Sci Am 252:110–117

Jorgensen JD (1978) Compression mechanisms in α-quartz structures – SiO_2 and GeO_2. J Appl Phys 49:5473–5478

King HE, Finger LW (1979) Diffracted beam crystal centering and its application to high-pressure crystallography. J Appl Crystallogr 12:374–378

Lehmann MS, Larsen FK (1974) A method for location of the peaks in step-scan-measured Bragg reflections. Acta Crystallogr A30:580–584

Levien L, Prewitt CT (1981) High-pressure crystal structure and compressibility of coesite. Am Mineral 66:324–333

Levien L, Prewitt CT, Weidner DJ (1980) Structure and elastic properties of quartz at pressure. Am Mineral 65:920–930

Robinson K, Gibbs GV, Ribbe PH (1971) Quadratic elongation: a quantitative measure of distortion in coordination polyhedra. Science 172:567–570

Simonov MA, Belov NV (1976) Crystal structures of bertrandite $Be_4[Si_2O_7](OH)_2$ and hemimorphite (calamine) $Zn_4[Si_2O_7](OH)_2H_2O$. Sov Phys Dolk 21:607–608

Solov'eva LP, Belov NV (1965) Precise determination of the crystal structure of bertrandite $Be_4[Si_2O_7](OH)_2$. Sov Phys Crystallogr 9:458–460

Zachariasen WH (1967) A general theory of X-ray diffraction in crystals. Acta Crystallogr 23:558–564

Zachariasen WH (1972) Refined crystal structure of phenacite Be_2SiO_4. Sov Phys Crystallogr 16:1021–1025

Received July 29, 1985